



Phenol removal onto novel activated carbons made from lignocellulosic precursors: Influence of surface properties

J.M. Valente Nabais^{a,*}, J.A. Gomes^a, Suhas^a, P.J.M. Carrott^a, C. Laginhas^a, S. Roman^b

^a Centro de Química de Évora & Departamento de Química, Universidade de Évora, Rua Romão Ramalho number 59, 7000-671 Évora, Portugal

^b Departamento de Física Aplicada, Universidad de Extremadura, 06071, Badajoz, Spain

ARTICLE INFO

Article history:

Received 27 November 2008

Received in revised form 19 January 2009

Accepted 19 January 2009

Available online 30 January 2009

Keywords:

Phenol
Activated carbon
Adsorption
Porosity
Wastewater treatment

ABSTRACT

The adsorption of phenol from dilute aqueous solutions onto new activated carbons (AC) was studied. The novel activated carbon was produced from lignocellulosic (LC) precursors of rapeseed and kenaf. Samples oxidised with nitric acid in liquid phase were also studied. The results have shown the significant potential of rapeseed and kenaf for the activated carbon production. The activated carbons produced by carbon dioxide activation were mainly microporous with BET apparent surface area up to $1350\text{ m}^2\text{ g}^{-1}$ and pore volume $0.5\text{ cm}^3\text{ g}^{-1}$. The effects of concentration (0.1–2 mM) and pH (3–13) were studied. The phenol adsorption isotherms at $25\text{ }^\circ\text{C}$ followed the Freundlich model with maximum adsorption capacities of approximately 80 and 50 mg g^{-1} for the pristine and oxidised activated carbons, respectively. The influence of pH on the adsorption has two trends for pH below and above 10. It was possible to conclude that when phenol is predominantly in the molecular form the most probable mechanism is based on the π – π dispersion interaction between the phenol aromatic ring and the delocalised π electrons present in the activated carbon aromatic structure. When phenolate is the major component the electrostatic repulsion that occurs at high pH values is the most important aspect of the adsorption mechanism.

© 2009 Elsevier B.V. All rights reserved.

1. Introduction

Lignocellulosics (LC) are widely used raw materials for activated carbon (AC) production with wood and coconut shell being the major precursors, and accounting for more than 165,000 ton/year of AC production [1]. Besides these commonly used raw materials, a number of lignocellulosic agricultural by-products such as eucalyptus wood, almond shell, vetiver grass, peanut shells, coir pith, chest nut, pistachio-nut shells, corncobs and palm stones have also been investigated for the production of ACs [2–9]. The search for new precursors is needed in order to produce activated carbons from low cost materials, such as industrial and agricultural residues. Our research group has also been working on some lignocellulosic materials like cork and coffee endocarp [10–12].

In the present study two lignocellulosic precursors, kenaf (*Hibiscus cannabinus*) and rapeseed (*Brassica napus*), were used for the production of ACs and the influence of the surface properties of the ACs on the adsorption of phenol was investigated. Phenol is an important toxic material listed as a priority pollutant by the US Environmental Protection Agency (EPA) [13], and also by the EU. The 80/778/EEC directive of the European Commission states

a maximum admissible concentration of $0.5\text{ }\mu\text{g l}^{-1}$ for phenol in water intended for human consumption. Phenol is considered to be very toxic to humans through oral exposure with symptoms including muscle weakness and tremors, loss of coordination, paralysis, convulsions, coma, liver and kidney damage, headache, fainting and other mental disturbances. The ingestion of 1 g has been reported to be lethal. Inhalation and dermal exposure to phenol is highly irritating to the skin, eyes, and mucous membranes in humans.

Phenol is the basic structural unit for a variety of synthetic organic compounds. It usually enters water sources from various chemical, pesticide, paper and pulp and dye manufacturing industries. Also, the wastewater from other industries such as gas and coke, resin, tanning, textile, plastic, rubber, pharmaceutical and petroleum contain different types of phenols. Besides industrial activity, wastewaters also contain phenols formed as a result of decay of vegetation. In view of the wide prevalence of phenol in different wastewaters and its toxicity to human and animal life even at low concentration, it is essential to remove it before discharge of wastewater into water bodies. Various methodologies have been designed for removal of phenols but among them adsorption using activated carbons is the one most frequently used. It is worthwhile pointing out that despite a vast number of studies including ACs from LCs the mechanism and influence of various factors affecting the phenol uptake is still not clear.

* Corresponding author. Tel.: +351 266745318; fax: +351 255745303.
E-mail address: jvn@uevora.pt (J.M.V. Nabais).

Nomenclature

| | |
|------------------|---|
| A_{BET} | BET apparent surface area ($\text{m}^2 \text{g}^{-1}$) |
| ACs | activated carbons |
| A_{ext} | external area ($\text{m}^2 \text{g}^{-1}$) |
| β | width at half height corrected for instrumental broadening |
| C_e | equilibrium concentration (mmol g^{-1}) |
| d_{002} | interplanar spacing (nm) |
| DR | Dubinin–Radushkevich method |
| K_f and n | characteristic constants of the Freundlich model |
| L_a | microcrystallite width (nm) |
| L_c | microcrystallite height (nm) |
| N_p | mean number of layer planes |
| pzc | point of zero charge |
| q_e | amount adsorbed at equilibrium (mg g^{-1}) |
| V_s | micropore volume given by α_s method ($\text{cm}^3 \text{g}^{-1}$) |
| V_0 | micropore volume given by DR method ($\text{cm}^3 \text{g}^{-1}$) |
| XRD | X-ray powder diffraction |

In general the uptake of an adsorbate (e.g. phenol) from aqueous solutions by ACs depends on various factors which include type of precursor for AC production, physical nature (surface area, pore size, pore volume, ash content, particle size) and functional groups present on the adsorbent, nature of adsorbate (pK_a , polarity, molecular weight, size, solubility) and on adsorbate solution conditions (pH, concentration, temperature).

This study has been undertaken with the aim of producing activated carbon from rapeseed and kenaf for the purpose of studying the adsorption of phenol on these materials. Also, the influence of the surface properties on phenol adsorption on the activated carbon produced was investigated. As evident from the literature, and to the best of our knowledge no research involving kenaf or rapeseed has apparently been reported on these objectives.

2. Experimental

2.1. Materials

The activated carbon samples were produced from two lignocellulosic precursors, kenaf (*H. cannabinus*) and rapeseed (*B. napus*). The physical activation with carbon dioxide as activating agent was done in a horizontal tubular furnace with heating rate of $10^\circ\text{C min}^{-1}$. Carbonisation was carried out for 1 h by heating to 400°C under a constant N_2 flow of $85 \text{ cm}^3 \text{ min}^{-1}$. Activation was carried out at 700°C under a CO_2 flow of $85 \text{ cm}^3 \text{ min}^{-1}$, for different times in order to obtain burn-offs between 20 and 80 wt%, indicated in the samples designation after C7 or K7, respectively, for activated carbon from rapeseed or kenaf, switching back to the N_2 flow and allowing to cool below 50°C before removing the AC from the furnace. The samples were washed with 150 cm^3 of distilled water for 24 h with stirring at room temperature. The samples were oven dried at 110°C for 24 h and stored on sealed flasks. Samples K748 and C738 were oxidised in liquid phase with concentrated nitric acid during 1 h in a hot plate with stirring at $80\text{--}90^\circ\text{C}$. The ACs were removed and washed with distilled water until the wash water attained the same pH value as the distilled water employed in the wash. The oxidised samples were designated as C738Ox and K748Ox.

2.2. Materials characterisation

Nitrogen adsorption isotherms at 77 K were determined using a CE Instruments Sorptomatic 1990 after outgassing the samples at

400°C to a residual vacuum of 5×10^{-6} mbar. Elemental analysis of carbon, hydrogen, sulfur, nitrogen and oxygen was carried out using a Eurovector EuroEA elemental analyser. The ash content was determined using the ASTM D2866–94 procedure and the point of zero charge (pzc) was determined by mass titrations using three suspensions with 7% (w/v) in carbon material with initial pH of 3, 6, and 11; the three initial pH values were obtained by adjusting the pH of a solution NaNO_3 0.1 M with NaOH or HNO_3 solutions, more details given elsewhere [14]. X-ray powder diffraction (XRD) patterns were determined using a Bruker AXS D8 advance diffractometer with Cu $K\alpha$ radiation ($\lambda = 0.150619 \text{ nm}$) at a step size of 0.020° between 5.000° and 60.020° . The precursor's content in cellulose and lignin was done by Agroleico (Porto Salvo, Portugal) using Portuguese Standards NP2029 and ME-414, respectively.

2.3. Phenol adsorption

A 1×10^{-2} M phenol stock solution was prepared from phenol (>99%, Aldrich). Batch adsorption experiments were carried out in test tubes of 50 cm^3 covered with rubber stoppers inserted into a shaking thermostat bath for 7 days. Each test tube contained 0.01 g of AC and 10 cm^3 of an appropriated phenol solution. The effects of concentration (0.1–2 mM) and pH (3–13) were studied. The quantification of the phenol in the liquid phase was carried out using a Thermo UV–vis spectrophotometer at 270 nm.

3. Results and discussion

3.1. Materials characterisation

The precursors before used were air dried, crushed and sieved in order to standardize the granulometry and homogenise the raw material. In the present work we used the 2–4 mm fraction for the ACs production. As can be seen in Table 1, the precursors have slight differences concerning the cellulose and lignin content. Kenaf has higher cellulose and lower lignin content than rapeseed. The elemental composition and ash content, besides having normal and expected values for this type of lignocellulosic materials, are very similar for the two used precursors.

The textural and chemical characterisation of the produced ACs can be seen in Table 2. All ACs have basic properties with pzc values between 9.14 and 9.98. The point of zero charge is defined by the pH value at which the total surface charge is zero. The samples produced from rapeseed have slightly smaller pzc values when compared to samples produced from kenaf with similar burn-off degree or activation time.

It is well known that the most relevant heteroatoms for the adsorption of phenol are nitrogen and oxygen [15]. All samples have moderate nitrogen content, around 1wt%, but noteworthy oxygen content which doesn't follow a specific trend with increasing sample burn-off, as can be seen from the data shown in Table 2. The oxygen content of each AC sample is the sum of several factors, namely the oxygen content of the precursor, the oxygen released during the heating process and the oxygenated functional groups introduced by the reaction between carbon dioxide and the carbon surface. Therefore, along the same sample series fluctuations occur with increasing burn-off.

The porous development of the produced ACs is very interesting. As shown in Table 2 the apparent BET surface area reaches the maximum value of 1352 and $1036 \text{ m}^2 \text{ g}^{-1}$ for rapeseed and kenaf samples, respectively. The AC samples have a low to moderate external area (A_{ext}), given by the α_s method and, for the same burn-off degree, samples from rapeseed have higher values of external area than the samples produced from kenaf. All samples are microporous, as indicated by the shape of the nitrogen adsorption

Table 1
Precursor characterisation.

| Precursor | Elemental composition (wt%) | | | | | Ash (wt%) | Cellulose (wt%) | Lignin (wt%) |
|-----------|-----------------------------|------|------|--------------|----------------|-----------|-----------------|--------------|
| | C | H | N | S | O ^b | | | |
| Kenaf | 41.01 | 5.05 | 1.46 | ^a | 49.69 | 2.80 | 41.7 | 10.9 |
| Rapeseed | 42.81 | 5.67 | 1.59 | ^a | 47.39 | 2.54 | 34.3 | 12.2 |

^a <Detection limit.^b By difference (100 – (%C + %H + %N + %S + Ash)).

isotherms at 77 K (not shown here for simplicity) which are all type I according to the IUPAC classification [16]. The difference between the pore volumes given by the α_s and Dubinin–Radushkevich (DR) methods, V_s and V_0 , respectively, can provide an estimate of the primary and secondary micropore volume considering the α_s volume as the total pore volume and the DR pore volume as an indication of the primary micropores. As shown in Table 2, all samples have very similar or equal values for both volumes which indicate that most of the pores present in the AC samples are narrow micropores, as confirmed by the mean pore width calculated by DFT methods. The calculated values for the samples used on the phenol adsorption are 1.23, 0.89, 1.18 and 1.06 nm for samples C738, C738Ox, K748 and K748Ox, respectively.

The sample modification by liquid phase oxidation with nitric acid, samples C738Ox and K748Ox, had produced drastic alterations to the surface chemistry of the samples, as indicated by the pzc values that changed from 9.63 to 2.32 and from 9.98 to 2.05 for samples C738 and K748, respectively. The modification with nitric acid has been reported in the literature in several papers. This procedure leads to the formation of a number of functional groups, namely lactones, carboxylic acid and anhydride, phenol and carbonyl groups, on the surface of the material [17,18].

The impact of the nitric acid treatment on the porosity was much less noticeable. It caused a slightly decrease in the apparent BET surface area and pore volume. As can be seen in Table 2, the apparent BET surface area decreased by approximately 25% and 15% for C738 and K748, respectively. The decrease in pore volume was also bigger for C738 than for K748. However, the opposite trend was observed for the external area of both samples. The results show that ACs from kenaf are more resistant to nitric acid treatment in liquid phase in regard to the sample pore properties. It seems that for K748 the nitric acid treatment undertaken results in a more extensive depletion of the materials external area with much less impact on their pore structure.

Nevertheless, we can state that the main goal of the nitric acid treatment carried out, to produce samples with very dif-

ferent surface chemistry but similar pore structure, was fully achieved.

The XRD patterns of carbon materials typically show two broad bands due to reflections from the (002) and (10) planes. From the position of the (002) band we can calculate an estimate of the interplanar spacing, d_{002} , by the application of Bragg's Law. Estimates of the mean microcrystallite dimensions can generally be obtained by using the Debye–Scherrer equations and the data from the bands (002) and (10), namely the position, θ , and the width at half height corrected for instrumental broadening, β . When applied to carbon materials the equations take the forms [19]:

$$L_c = 0.90\lambda/\beta \cos \theta_{002} \quad (1)$$

$$L_a = 1.94\lambda/\beta \cos \theta_{10} \quad (2)$$

The L_c and L_a values give an estimate of the microcrystallites height and width, respectively. Also the mean number of layer planes in the microcrystallites (N_p) can be estimated using the ratio L_c/d_{002} .

As can be seen in Fig. 1, the XRD patterns of samples C738 and K748, show the typical bands due to reflections from the (002) and (10) planes, but also show other peaks due to the presence of various heteroatoms. Some of those peaks are overlapping the bands (002) and (10). For that reason, the correct assessment of the characteristics needed to calculate the estimate of the microcrystallite dimension is difficult and most of the times not possible. This difficulty is greater for ACs from rapeseed. Nevertheless, for samples from Kenaf it is possible to calculate the estimate which indicates that K samples have interplanar spacing between 0.353 and 0.367 nm, L_c in the range 0.716–0.832 nm and L_a values sandwiched between 2.06 and 2.30 nm.

We also tried to identify the heteroatoms present in the samples by using the best match possible between the peaks shown on the XRD pattern of each sample (see Fig. 1) and the patterns of the existing database of powder diffraction files included in the software DIFFRAC^{plus}®. It is clearly visible in Fig. 1 that sample C738

Table 2
Textural and chemical characterisation of the activated carbons from kenaf and rapeseed.

| Sample | Porosity | | | | pzc | Ash (wt%) | Elemental composition (wt%) | | | |
|--------|---------------------------------|-------------------------|----------------------------|-------------------------|------|-----------|-----------------------------|-------|------|------|
| | BET, A_{BET} ($m^2 g^{-1}$) | α_s | | DR | | | O ^b | C | H | N |
| | | V_s ($cm^3 g^{-1}$) | A_{ext} ($m^2 g^{-1}$) | V_0 ($cm^3 g^{-1}$) | | | | | | |
| C4 | ^a | ^a | ^a | ^a | 9.76 | 9.96 | 15.42 | 70.93 | 2.10 | 1.59 |
| C720 | 624 | 0.27 | 67 | 0.26 | 9.27 | 10.3 | 12.67 | 76.06 | 0.36 | 0.64 |
| C738 | 1112 | 0.52 | 126 | 0.47 | 9.63 | 12.2 | 6.52 | 80.31 | 0.28 | 0.64 |
| C738Ox | 827 | 0.35 | 78 | 0.35 | 2.32 | 0.91 | 20.32 | 75.31 | 2.32 | 1.14 |
| C766 | 1224 | 0.53 | 231 | 0.51 | 9.71 | 16.2 | 11.20 | 71.00 | 0.38 | 1.21 |
| C781 | 1352 | 0.54 | 242 | 0.57 | 9.14 | 17.6 | 10.79 | 69.99 | 0.35 | 1.25 |
| K4 | ^a | ^a | ^a | ^a | 9.96 | 9.72 | 15.14 | 72.09 | 1.69 | 1.36 |
| K722 | 781 | 0.39 | 19 | 0.34 | 9.73 | 8.93 | 13.05 | 76.33 | 0.49 | 1.20 |
| K731 | 867 | 0.39 | 32 | 0.37 | 9.72 | 10.2 | 12.88 | 75.29 | 0.48 | 1.10 |
| K748 | 1021 | 0.45 | 84 | 0.45 | 9.98 | 14.9 | 17.70 | 65.73 | 0.29 | 1.30 |
| K748Ox | 962 | 0.45 | 20 | 0.41 | 2.05 | 0.65 | 23.37 | 72.03 | 2.46 | 1.49 |
| K776 | 1036 | 0.47 | 43 | 0.43 | 9.71 | 11.9 | 22.63 | 63.34 | 0.39 | 1.76 |

^a Null adsorption of N_2 at 77 K.^b By difference (100 – (%C + %H + %N + %S + Ash)).

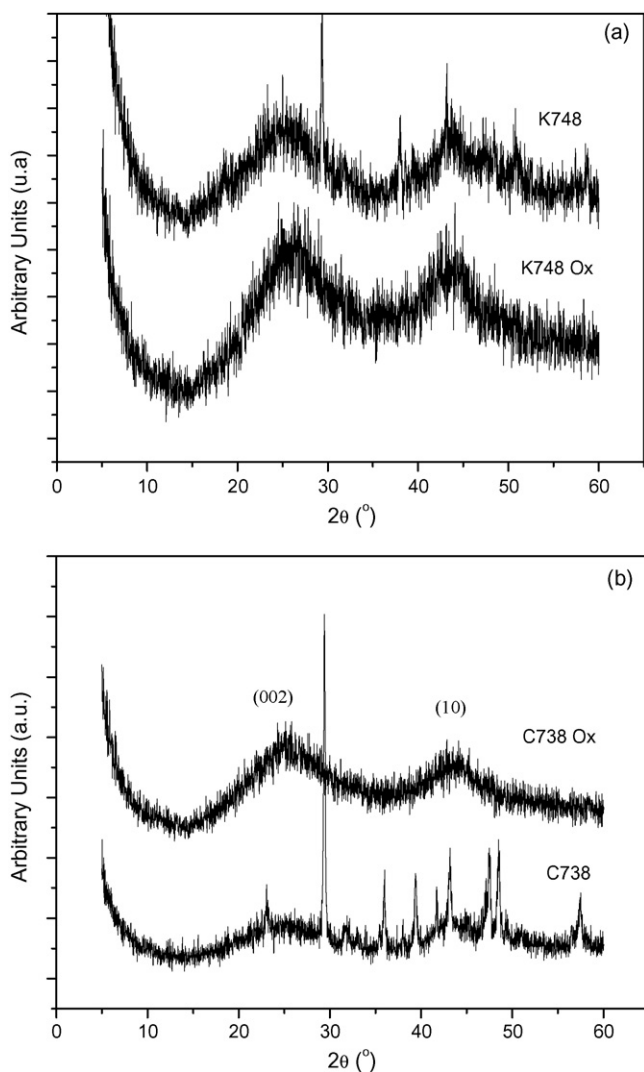


Fig. 1. Representative XRD patterns. (a) Samples K748 and K748Ox. (b) Samples C738 and C738Ox.

has a more heterogeneous surface with the identification of the possible presence of Na, Ti, Al, Mg, K, Si, Fe, Pb and Sn in several possible oxide forms. Sample K748 has a much more homogeneous XRD pattern with the possible presence of Na, Al, Mg, Si and Pb as heteroatoms.

It is clearly visible in Fig. 1 that for samples C738Ox and K748Ox all peaks attributed to the presence of heteroatoms are missing in consequence of their removal by the nitric acid treatment. This treatment besides having direct effect on the surface functional groups, as shown before, also has a significant impact on the surface heterogeneity by leaching out almost all of the heteroatoms besides oxygen and hydrogen.

3.2. Phenol adsorption

For the study of the phenol adsorption from dilute aqueous solutions we selected four samples, C738, C738Ox, K748 and K748Ox, from different precursors and with different surface properties to evaluate the potential of the produced ACs to be used for the phenol removal and to understand the influence of the surface characteristics on the adsorption process. Fig. 2 shows the phenol adsorption isotherms at 25 °C.

Phenol can be considered as a weak acid with a pK_a value of 9.95. For pH values below the pK_a value the predominant specie in

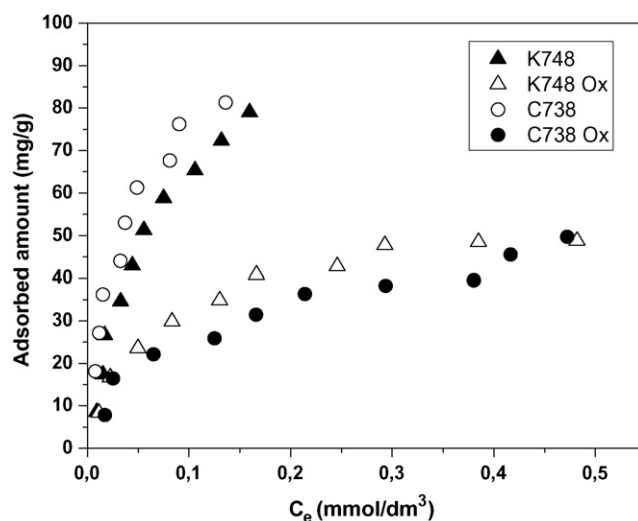


Fig. 2. Phenol adsorption isotherms at 25 °C (units mg g^{-1} and mmol dm^{-3}).

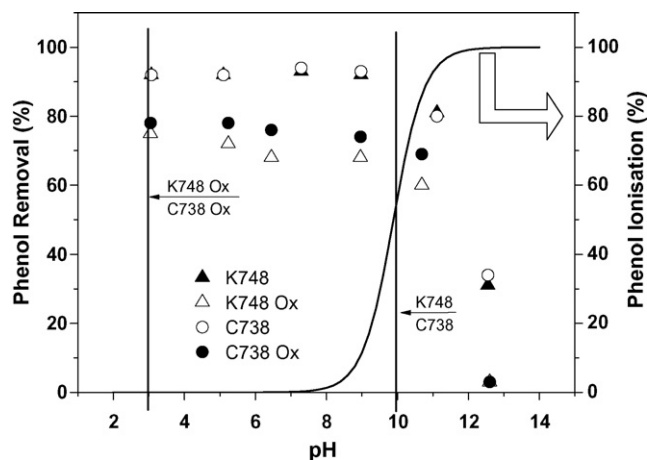
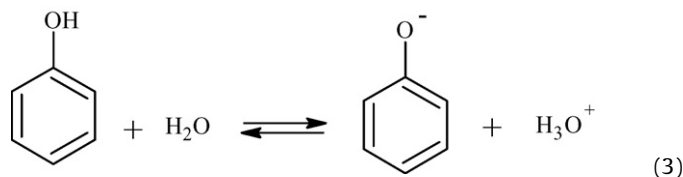


Fig. 3. Phenol removal as function of the initial solution pH.

solution is the molecular form of phenol. For pH above this value the aromatic ring becomes partially negatively charged by means of the hydroxyl group ionisation (see Eq. (3)). In consequence, the ionic form is predominant for pH values higher than 9.95. The phenol ionisation curve can be seen in Fig. 3.



The shape of the isotherms is the first experimental tool to analyse the adsorption process and diagnose the nature of the adsorption. The most common isotherm types can be classified according to the Giles classification [20] or according to other phenomenological aspects of the adsorption [21]. Using the last classification the isotherms shown in Fig. 2 can be classified as F Type, which indicates adsorption on heterogeneous surfaces. According to the Giles classification, which is the one largely used in the literature, all isotherms can be classified as type L suggesting that the aromatic ring adsorbs parallel to the surface and no strong competition exists between the adsorbate and the solvent to occupy the adsorption site. Each isotherm type can be subdi-

Table 3
Freundlich Constants for the uptake of phenol.

| Sample | K_f (mg g ⁻¹) | n | r^2 |
|--------|-----------------------------|-----|-------|
| C738 | 84.1 | 2.7 | 0.984 |
| C738x | 57.0 | 2.0 | 0.979 |
| K748 | 82.6 | 1.9 | 0.986 |
| K748x | 63.1 | 2.7 | 0.981 |

vided into subgroups related to the adsorption behaviour at higher concentrations. Isotherms of samples C748 and K738 can be considered as L1, the isotherm of sample K748Ox as L2 and the isotherm of sample C738Ox as L3.

The C738Ox isotherm shows a step at approximately $C_e = 0.4 \text{ mmol g}^{-1}$ which was attributed by other authors to a change from horizontal to vertical orientations of the adsorbed molecule [22]. If we take this into consideration, and also consider this step as the saturation of the AC surface for adsorbing phenol in a horizontal orientation, then a rough estimate of the number of microcrystallites can be done for sample C738Ox. The step corresponds to a saturation point of 35 mg of phenol per AC gram (see Fig. 2). Using this value and the value 0.522 nm^2 for the phenol molecular area in a horizontal adsorption orientation [15] and the data from XRD, namely the N_p , L_a and L_c values, to evaluate the total area accessible to phenol adsorption (4.287 nm^2) one can calculate the estimate of 2.72×10^{19} microcrystallites per gram of AC. Despite all the drawbacks of this estimate we believe it is worthwhile to carry out the exercise.

The pH value of the dilute aqueous phenol solution used for the determination of the isotherms, was approximately 7.5 for all concentrations which indicates that phenol is predominantly in the molecular form. Therefore, dispersive interactions were expected to be the most relevant driving force for the adsorption of phenol. Taking this into consideration, the superior phenol adsorption of sample C738 when compared with sample K748 can be explained by the effect of the higher oxygen content of sample K748 that lead to a weaker interaction between phenol and the carbon surface (see Table 2). A more detailed explanation of this effect can be found when the pH influence is discussed. The same reason is expected to describe the reduced adsorption capacity of the oxidised sample.

The results were analysed using the Freundlich isotherm in the linear form as given by Eq. (4):

$$\log q_e = \log k_f + \frac{1}{n} \log C_e \quad (4)$$

where C_e is the equilibrium concentration, q_e is the amount adsorbed at equilibrium, K_f and n are characteristic constants. Typically, n is related to the enthalpy and intensity of adsorption and the quantity K_f is the amount adsorbed at $C_e = 1 \text{ mmol dm}^{-3}$ [23]. The characteristic constants listed in Table 3 were calculated from the best-fit lines to the experimental data.

The comparison of K_f values with other published papers must be carefully done as it depends on the concentration units used which means that K_f is not a measure of the maximum adsorption capacity. Thus, this value can only be used as a comparative measure under specific conditions [23,24]. Nevertheless, the K_f values obtained by us for AC pristine samples can be favourably compared with other published papers [25–28]. The n values obtained indicate that the adsorption process is favourable from the thermodynamic point of view.

The adsorption capacity for the pristine and oxidised activated carbons can be estimated from the isotherms shown in Fig. 2. It can be seen that for the oxidised samples the isotherms show a plateau at approximately 50 mg g^{-1} , for C738 and K748 the adsorption capacity is about 80 mg g^{-1} . The comparison of our results with results already published shows that the performance of the activated carbons tested can be considered very good. Stavropoulos

et al. [17] and Singh et al. [32] reported phenol adsorption up to 35 mg g^{-1} . Din et al. [25] and Villacañas et al. [18] published slightly higher values, between 60 and 150 mg g^{-1} .

As can be seen in Fig. 2 the oxidised samples have much less adsorption capacity when compared with the pristine sample. The lower adsorption capacity of the oxidised samples cannot be explained only by the porosity modification of the samples. The performance of the oxidised samples can be attributed to two different reasons. On one hand for the oxidised samples it is more difficult to displace the solvent molecules (water) from the AC surface in order to adsorb phenol due to the possibility of hydrogen bond formation between the surface oxygen groups and the water molecules. On the other hand, the functionalisation of the AC surface by nitric acid oxidation lead to a smaller electronic density of the basal planes, which are accessible to phenol adsorption, due to a stronger localisation of the π electrons at the ACs graphene layers. When phenol is predominantly in the molecular form the adsorption occurs mainly via the π - π dispersion interaction between the π delocalised electrons on the ACs graphene layers and the aromatic ring of the phenol molecule. Therefore, the increase in oxygen content, included in the oxygenated surface functional groups, leads to a decrease in this interaction as it tends to localise the π electrons of the graphene layers.

The study of the influence of initial solution pH on the phenol adsorption can be seen in Fig. 3. The vertical lines correspond to the pzc of the carbons and designate the turning point of the ACs mean surface charge. For pH values situated on the left side and on the right side of the lines the ACs have positive and negative charge, respectively. The increasing distance from the vertical lines corresponds to surfaces with greater charge density, as the difference between the pH and pzc values is also bigger. The phenol ionisation curve is also inserted in Fig. 3.

As can be seen in Fig. 3 the phenol adsorption decreases with pH. We can observe two distinct areas or behaviour, the first one for pH values less than 10 where the phenol removal only shows a slight decrease. The second trend is observed for pH values higher than 10 with the occurrence of a noteworthy decrease in the phenol removal. The same trend was also observed by Hameed and Rahman [28].

It is well known that phenol adsorption onto activated carbon can occur via a complex interplay of electrostatic and dispersion interactions with three possible mechanisms:

- π - π dispersion interaction between the phenol aromatic ring and the delocalised π electrons present in the aromatic structure of the graphene layers, proposed by Coughlin and Ezra [29];
- hydrogen bond formation proposed by Coughlin and Ezra [29];
- electron donor-acceptor complex formation at the carbon surface where the oxygen of the surface carbonyl group acts as the electron donor and the phenol aromatic ring as the acceptor, proposed by Mattson et al. [30].

Probably the global adsorption process involves more than one possible mechanism. In addition, electrostatic interactions can play a significant role if phenol is predominately in the phenolate ion form that can interact with the charged AC surface. Both aspects are determined by the solution pH in relation to phenol pK_a and the AC point of zero charge.

It is clear that mechanisms 1 and 3 cannot occur simultaneously as the presence of one excludes the possibility of the other. The first mechanism states that the presence of oxygen leads to a phenol adsorption decrease by a weaker interaction between the AC π electrons and phenol, as oxygen groups act as activating groups which are electron-withdrawing groups and tend to promote a greater charge and electron localisation of the aromatic system at the graphene layers. According to mechanism 3 those functional

groups will lead to an increase in the adsorption capacity by the formation of the electron donor–acceptor complex. In our case the most probable mechanism is the π – π dispersion interaction mechanism as we have observed a decrease in the phenol adsorption for the oxidised samples.

When the π – π dispersion interaction is the main adsorption mechanism the most probable is that the phenol molecule is adsorbed in the flat position and when the electrostatic interaction is the predominant mechanism the molecule is adsorbed in the vertical position. Other possible mechanisms were also proposed such as the formation of phenol oligomers [31] and polymers [27] on the surface of the carbon material. However, those mechanisms have more probability to occur when carbon black is used.

Besides the mean surface charge (positive or negative) we should also take into account the extent of the surface functional groups ionisation, which is related to the surface coverage by the charged groups and to the charge density of the surface. This extent can be assessed by the difference between pzc and solution pH, the bigger the difference the higher the negative charge on the surface.

The effect of initial solution pH on the phenol adsorption can be explained taking into account all the previously mentioned mechanisms and interactions. For pH below 10 phenol is predominately in the molecular form and thus the electrostatic interactions do not have a significant role on the adsorption. That is why we cannot observe, with the pH increase from 3 to 10, a higher decrease in the adsorption for samples C738Ox and K748Ox, which have a negatively charged surface or a increase in the adsorption for samples C738 and K748, which have a positive surface charge. In this zone the driving force for the adsorption is the dispersive interactions which are not determined by the electric nature of the surface. The oxidised samples have smaller adsorption capacity due to the effect of the oxide functional groups inserted on the ACs surface. For pH above 10 the phenolate ion became the predominant species in solution and hence the electrostatic repulsion between the phenolate and the negatively charged ACs surface leads to a significant decrease in the phenol adsorption. This decrease is more relevant for samples C738Ox and K748Ox as these samples have a higher charge density caused by a more extensive ionisation of the functional groups indicated by the bigger difference between solution pH and the ACs point of zero charge.

4. Conclusion

In conclusion or final comment we would like to mention the following topics:

- The use of rapeseed and kenaf as precursors for activated carbon production is very motivating. All activated carbons produced in this study have basic properties with point of zero charge values higher than 9 and a well developed porous structure. For instance, the apparent BET surface area reaches the maximum value of 1352 and 1036 m² g⁻¹ for rapeseed and kenaf samples, respectively.
- The modification by liquid phase oxidation with nitric acid produced drastic alterations to the samples surface chemistry but only a small impact on their porosity properties. The value of the point of zero charge after the treatment decreased from 9.63 to 2.32 and from 9.98 to 2.05 for samples C738 and K748, respectively. Concerning the effect on the porosity of the samples we can conclude that activated carbon from kenaf are more resistant to nitric acid treatment. In this case the treatment results in a more extensive depletion of the material external area without having a significant impact on the pore volume.
- The phenol adsorption at 25 °C reveals that oxidised samples have much less adsorption capacity than the corresponding pristine activated carbon because the increased acidity of oxidised sam-

ples leads to an intensity decrease in the adsorption driving force, which is based on the π – π dispersion interaction between the π delocalised electrons on the activated carbon graphene layers and the aromatic ring of the phenol molecule.

- The phenol adsorption for pH less than 10 is independent of the solution pH. On the other hand, for pH values higher than 10 a noteworthy decrease in the phenol removal was observed. Therefore, we can conclude that phenol adsorption occurs via two possible mechanisms being the first one attributed to the adsorption by means of dispersive interactions between the phenol aromatic ring and the activated carbon aromatic structure. In this case the electrostatic interactions don't have a significant role on the adsorption. The second mechanism, which is based on the dispersive attractive forces and the electrostatic repulsion interactions, occurs when phenol is predominantly in the phenolate form and the activated carbon surface is negatively charged.
- We can also conclude that activated carbons from rapeseed and kenaf are promising materials to be used for contaminated water treatment as the obtained results can be favourably compared with other reported papers.

Acknowledgements

The authors are grateful to the Fundação para a Ciência e Tecnologia (Portugal) and the European Regional Development Fund (FEDER) for financial support (Project PTDC/CTM/66552/2006).

References

- [1] R.C. Bansal, J.-B. Donet, S. Fritz, Active Carbon, Marcel Dekker, New York, 1988.
- [2] M.A. Lillo-Ródenas, J.P. Marco-Lozar, D. Cazorla-Amorós, A. Linares-Solano, Activated carbons prepared by pyrolysis of mixtures of carbon precursor/alkaline hydroxide, *Journal of Analytical and Applied Pyrolysis* 80 (2007) 166–174.
- [3] S. Gaspard, S. Altenor, E.A. Dawson, P.A. Barnes, A. Ouensanga, Activated carbon from vetiver roots: gas and liquid adsorption studies, *Journal of Hazardous Materials* 144 (2007) 73–81.
- [4] K. Wilson, H. Yang, C.W. Seo, W.E. Marshall, Select metal adsorption by activated carbon made from peanut shells, *Bioresource Technology* 97 (2006) 2266–2270.
- [5] C. Namasivayam, D. Sangeetha, Recycling of agricultural solid waste, coir pith: removal of anions, heavy metals, organics and dyes from water by adsorption onto ZnCl₂ activated coir pith carbon, *Journal of Hazardous Materials* 135 (2006) 449–452.
- [6] V. Gómez-Serrano, E.M. Cuerda-Correa, M.C. Fernández-González, M.F. Alexandre-Franco, A. Macías-García, Preparation of activated carbons from chestnut wood by phosphoric acid-chemical activation. Study of microporosity and fractal dimension, *Materials Letters* 59 (2005) 846–853.
- [7] T. Yang, A.C. Lua, Characteristics of activated carbons prepared from pistachio-nut shells by physical activation, *Journal of Colloid and Interface Science* 267 (2003) 408–417.
- [8] A.-N.A. El-Hendawy, S.E. Samra, B.S. Girgis, Adsorption characteristics of activated carbons obtained from corncobs, *Colloids and Surfaces A: Physico-chemical and Engineering Aspects* 180 (2001) 209–221.
- [9] Z. Hu, H. Guo, M.P. Srinivasan, N. Yaming, A simple method for developing mesoporosity in activated carbon, *Separation and Purification Technology* 31 (2003) 47–52.
- [10] J.M.V. Nabais, P. Nunes, P.J.M. Carrott, M.M.L. Ribeiro Carrott, A.M. García, M.A. Díaz-Diez, Production of activated carbons from coffee endocarp by CO₂ and steam activation, *Fuel Processing Technology* 89 (2008) 262–268.
- [11] J.V. Nabais, P. Carrott, M.M.L. Ribeiro Carrott, V. Luz, A.L. Ortiz, Influence of preparation conditions in the textural and chemical properties of activated carbons from a novel biomass precursor: the coffee endocarp, *Bioresource Technology* 99 (2008) 7224–7231.
- [12] A. Domínguez, J.A. Menéndez, Y. Fernández, J.J. Pis, J.M.V. Nabais, P.J.M. Carrott, M.M.L.R. Carrott, Conventional and microwave induced pyrolysis of coffee hulls for the production of a hydrogen rich fuel gas, *Journal of Analytical and Applied Pyrolysis* 79 (2007) 128–135.
- [13] <http://www.epa.gov/waterscience/methods/pollutants.htm>.
- [14] P.J.M. Carrott, J.M.V. Nabais, M.M.L. Ribeiro Carrott, J.A. Menéndez, Thermal treatments of activated carbon fibres using a microwave furnace, *Microporous and Mesoporous Materials* 47 (2001) 243–252.
- [15] Carbon materials as adsorbents in aqueous solutions, in: L.R. Radovic, C. Moreno-Castillo, J. Rivera-Utrilla (Eds.), in: *Chemistry and Physics of Carbon*, vol. 27, Marcel Dekker Inc., New York, 2000, pp. 227–403.
- [16] J. Rouquerol, D. Avnir, C.W. Fairbridge, D.H. Everett, J.H. Haynes, N. Pernicone, J. Ramsay, K.S. Sing, K.K. Unger, Recommendations for the characterization of porous solids, *Pure and Applied Chemistry* 66 (8) (1994) 1739–1758.

- [17] G.G. Stavropoulos, P. Samaras, G.P. Sakellariopoulos, Effect of activated carbon modification on porosity, surface structure and phenol adsorption, *Journal of Hazardous Materials* 151 (2008) 414–421.
- [18] F. Villacanas, M.F.R. Pereira, J.M. Orfão, J.L. Figueiredo, Adsorption of simple aromatic compounds on activated carbons, *Journal of Colloid and Interface Science* 293 (2006) 128–136.
- [19] P.J.M. Carrott, J.M.V. Nabais, M.M.L. Ribeiro Carrott, J.A. Pajares, Preparation of activated carbon fibres from acrylic textile fibres, *Carbon* 39 (2001) 1543–1555.
- [20] C.H. Giles, D. Smith, A. Huitson, A general treatment and classification of the solute adsorption, *Journal of Colloid and Interface Science* 47 (1974) 755–765.
- [21] J. Lyklema, *Fundamentals of interface and colloid science Solid–liquid interfaces*, vol. 2, Academic Press, New York, 1995.
- [22] J.S. Mattson, H.B. Mark, *Activated Carbons*, Marcel Dekker, New York, 1971.
- [23] P.J.M. Carrott, P.A.M. Mourão, M.M.L. Ribeiro Carrott, E.M. Gonçalves, Separating surface and solvent effects and the notion of critical adsorption energy in the adsorption of phenolic compounds by activated carbons, *Langmuir* 21 (2005) 11863–11869.
- [24] P.A.M. Mourão, P.J.M. Carrott, M.M.L. Ribeiro Carrott, Application of different equations to adsorption isotherms of phenolic compounds on activated carbons prepared from cork, *Carbon* 44 (2006) 2422–2429.
- [25] A.T.M. Din, B.H. Hameed, A.L. Ahmad, Batch adsorption of phenol onto physicochemical-activated coconut shell, *Journal of Hazardous Materials*, doi:10.1016/j.hazmat.2008.05.009.
- [26] C. Moreno-Castilla, Adsorption of organic molecules from aqueous solutions on carbon materials, *Carbon* 42 (2004) 83–94.
- [27] N.S. Abuzaid, G.F. Nakhla, Effect of solution pH on the kinetics of phenolics uptake on granular activated carbon, *Journal of Hazardous Materials* 49 (1996) 217–230.
- [28] B.H. Hameed, A.A. Rahman, Removal of phenol from aqueous solutions by adsorption onto activated carbon prepared from biomass material, *Journal of Hazardous Materials*, doi:10.1016/j.hazmat.2008.03.028.
- [29] R.W. Coughlin, F.S. Ezra, Role of surface acidity in the adsorption of organic pollutants on the surface of carbon *Environ. Science Technology* 2 (4) (1968) 291–297.
- [30] J.S. Mattson, H.B. Mark Jr., M.D. Malbin, W.J. Weber Jr., J.C. Crittenden, Surface chemistry of active carbon: specific adsorption of phenols, *Journal of Colloid and Interface Science* 31 (1) (1969) 116–130.
- [31] Q. Lu, G.A. Sorial, The effect of functional groups on oligomerization of phenolics on activated carbons, *Journal of Hazardous Materials* 148 (2007) 436–445.
- [32] K.P. Singh, A. Malik, S. Sinha, P. Ojha, Liquid-phase adsorption of phenols using activated carbons derived from agricultural waste material, *Journal of Hazardous Materials* 150 (2008) 626–641.